Two-Dimensional Time-Dependent Vortex Regions Based on the Acceleration Magnitude

Jens Kasten, Jan Reininghaus, Ingrid Hotz, and Hans-Christian Hege, *Member, IEEE*

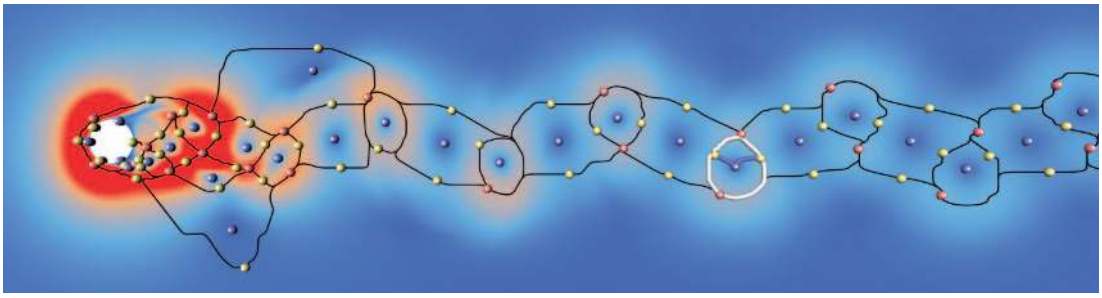

Fig. 1. This image shows one time slice of the cylinder dataset. Color represents the acceleration magnitude overlaid by its critical points and maxima lines connecting maxima with saddles. The topological skeleton is used to extract vortex regions defined as the region containing a vortex-like minimum bounded by maxima lines. The minima lines (blue) connecting minima with saddles are only displayed for the highlighted region.

Abstract—Acceleration is a fundamental quantity of flow fields that captures Galilean invariant properties of particle motion. Considering the magnitude of this field, minima represent characteristic structures of the flow that can be classified as saddle- or vortex-like. We made the interesting observation that vortex-like minima are enclosed by particularly pronounced ridges. This makes it possible to define boundaries of vortex regions in a parameter-free way. Utilizing scalar field topology, a robust algorithm can be designed to extract such boundaries. They can be arbitrarily shaped. An efficient tracking algorithm allows us to display the temporal evolution of vortices. Various vortex models are used to evaluate the method. We apply our method to two-dimensional model systems from computational fluid dynamics and compare the results to those arising from existing definitions.

Index Terms—Vortex regions, time-dependent flow fields, feature extraction.

1 Introduction

Vortices play a fundamental role for the understanding and analysis of complex fluid flows. Researchers are interested in the location, size, and strength of vortices as well as their temporal development and interaction. This interest is driven by questions like: What causes new vortices to arise or dissolve, to grow or shrink, to merge or split? Applications in which these tasks naturally arise include fundamental research on turbulent flows as well as specific design tasks, e.g., to improve the lift of an airfoil by controlling the flow behavior. Thereby two-dimensional flow fields still play a fundamental role [28, 32].

Despite its importance, there is no common mathematical definition of a vortex or vortex region. A variety of different approaches have been proposed in the past that define vortex cores and regions. For an overview over these methods, we refer to Sec. 2.

A fundamental quantity that indicates vortex-like behavior of particles is the acceleration. This Galilean invariant quantity represents the change of velocity and direction of a particle in time and is part of the Navier-Stokes equations. It was shown that the minima of its magnitude can be interpreted as time-dependent counterparts of critical points of standard vector field topology, which can be classified as vortex cores and saddles [13]. Analyzing the acceleration magnitude field further shows that vortex-like minima are enclosed by pronounced ridges, indicating the spatial extent of the vortex. This provides a basis for a consistent treatment of vortices: While a vortex core is defined at the position of a minimum, the corresponding basin, bounded by maximum lines, is interpreted as the associated vortex region, cf. Sec. 3.

This notion of vortices is entirely formulated in the context of scalar field topology and, thus, the full power of the corresponding algorithmic framework [21] can be exploited. This concerns robust extraction and tracking methods as well as a vortex hierarchy using a spatio-temporal importance measure based on persistence [22]. The hierarchy of the vortex core lines can be directly assigned to the regions.

In contrast to previous work, this novel definition of a vortex region combines the following three advantages:

1. It is Galilean invariant. The definition of the vortex regions is solely based on the acceleration, which is Galilean invariant. This is an essential property when dealing with time-dependent flows.

2. It allows for vortex regions of arbitrary shape. Using scalar field topology as the basis for the definition of vortex regions, the extraction algorithm is not restricted to star- or convex-shaped geometries.

3. It does not require any threshold or iso-value. This enables an unsupervised extraction of vortex regions in complex time-dependent datasets. This is important, e.g., for analyzing very large data sets.

The method is described in detail in Sec. 4 and 5. In Sec. 6, it is evaluated using model systems from computational fluid dynamics.

- *Jens Kasten is with Zuse Institute Berlin, E-mail: kasten@zib.de.*
- *Jan Reininghaus is with Zuse Institute Berlin, E-mail: reininghaus@zib.de.*
- *Ingrid Hotz is with Zuse Institute Berlin, E-mail: hotz@zib.de.*
- *Hans-Christian Hege is with Zuse Institute Berlin, E-mail: hege@zib.de.*

Manuscript received 31 March 2011; accepted 1 August 2011; posted online 23 October 2011; mailed on 14 October 2011.
For information on obtaining reprints of this article, please send email to: tvcg@computer.org.

The results are compared to other definitions of vortex regions and ridges of the finite time Lyapunov exponent (FTLE).

2 Related Work

The analysis of flow fields includes the extraction of vortices and their regions of influence, as these are the main structures in these fields. Despite its importance, no unique mathematical definition is available for these features. Thus, there exists a vast amount of publications dealing with vortex extraction and their definition. For a good overview, we refer to Post et al. [5, 19]. In addition, methods to analyze time-dependent vector fields were proposed. There are many promising approaches; we refer to Pobitzer et al. [18] for an extensive overview of the recent publications.

Extraction techniques for vortex regions can be divided in the following categories: First, there are approaches that use an indicator function related to vortical activity. Thereby, commonly used indicator quantities are vorticity magnitude, pressure, helicity, normalized helicity, λ_2 by Jeong et al. [12] or the Q quantity proposed by Hunt [10]. Recently, Haller proposed a feature identifier that is rotation invariant [9]. Since these measures indicate vortical activity, a vortex region can be defined through a threshold that distinguishes the influence region of the vortex from the rest of the domain. Iso-surface extraction can be used to visualize the region boundary. As a drawback, using iso-surface extraction, it is not possible to distinguish between nearby vortices, if their regions partially merge. Moreover, one has to choose a global threshold parameter, which is quite arbitrary, since there is only an intuitive notion of vortex activity for the mentioned quantities. Since some of the quantities define vortex strength, there may be no threshold value to extract the regions of both strong and weak vortices. As a remedy, Schneider et al. [25] proposed an extraction algorithm for vortex regions (based on λ_2) using the contour tree for the selection of the geometry. An exploratory technique to visualize time-dependent vortices in three-dimensions was introduced by Tikhonova et al. [30].

The second class of definitions of vortex regions uses the combination of a vortex indicator function and a geometrical extraction algorithm. Here, vortex regions are typically extracted for previously defined vortex core lines by sending out a fan of rays from the center. The rays are cut, if a certain criterion is met on the ray. The resulting regions are restricted to star-shaped geometries seen from the vortex core. These are not arbitrary star-shaped regions. Banks and Singer [1] introduced this method to construct a vortex hull as a series of connected contour lines. The contour line that connects the endpoints of the rays is the outer boundary of the vortex in that plane. They used a pressure threshold to mark the boundary of a vortex region induced by the length of the rays. Bauer et al. [3] used a threshold of the absolute value of the imaginary part of the complex eigenvalues of the Jacobian instead of the pressure threshold. Furthermore, Stegmaier et al. [27] used a threshold of λ_2 to determine the termination of the rays. Garth et al. [6] searched for local maxima of the tangential velocity component using the Rankine vortex model as a basis for their definition. Jankun-Kelly et al. [11] build an approach to robustly extract vortices based on local extrema of different scalar fields. They extract three-dimensional vortices using a predictor-corrector method and k-means clustering to find the correct extremal structures. The corresponding vortex regions are also based on the maximum tangential velocity. Note that their extracted vortex regions depend on the frame of reference, since velocity is Galilean variant.

The third category consists of approaches that use a purely geometric definition of vortex regions. Sadarjoen and Post [24] searched for streamlines with a winding angle of 2π. They restricted their definition to streamlines for which the distance of start end endpoint is "close". A clustering of streamlines belonging to the same vortex result in an elliptical representation of the vortex regions. Reinders et al. [20] extended the approach to 3D. Petz et al. [17] defined vortex regions searching for closed streamlines in rotated version of the vector field. They were able to build a hierarchy of these regions. All these approaches are not Galilean invariant, since they use streamlines that depend on the chosen frame of reference.

The tracking of vortices in time-dependent dataset is one of the main tasks for the analysis of non-stationary flow fields. Theisel et al. [29] proposed the "Feature Flow Field" approach to track the critical points of vector field topology. Their approach can also be used to extract the evolution of critical points of scalar field topology. Furthermore, Tricoche et al. [31] and Garth et al. [7] proposed a technique to track vector field singularities. Bauer and Peikert [2] presented a method for vortex core line extraction and tracking in scale-space. Reininghaus et al. [22] propose a combinatorial approach for tracking critical points in scalar fields.

3 Motivation

The basis of our considerations builds on the particle acceleration. In this section we motivate this choice and our definition of vortex regions for two-dimensional flow fields

Particle acceleration $\mathbf{a}$ is the material derivative of the flow field $\mathbf{v}$, i.e. the acceleration in a space-time point $(\mathbf{x},t)$ is given by

$$\mathbf{a}(\mathbf{x},t) = D\mathbf{v}/Dt = \partial_t \mathbf{v}(\mathbf{x},t) + (\mathbf{v}(\mathbf{x},t)\cdot\nabla)\,\mathbf{v}(\mathbf{x},t), \tag{1}$$

where ∂_t is the partial derivative with respect to t and ∇ the spatial gradient, i.e. (∂_x,∂_y) for the two-dimensional case. Knowing the acceleration and the initial velocity of a particle is sufficient to describe its trajectory. While the initial velocity changes under Galilean transformations, the acceleration is a Galilean invariant quantity and is therefore independent from the chosen frame of reference. As a part of the Navier-Stokes equations, it has the same invariances. Thus, the acceleration can be seen as one of the fundamental quantities describing particle motion.

Kasten et al. [13] have shown that the minima of the acceleration magnitude can be used to identify vortices in non-stationary flow fields. They found that minima of the acceleration magnitude can be interpreted as non-stationary counterparts to the critical points of vector field topology. This property can also be supported considering the Navier-Stokes equations. The incompressible equations are:

$$\mathbf{a}(\mathbf{x},t) = -\nabla p(\mathbf{x},t) + \nu\,\Delta\mathbf{u}(\mathbf{x},t) + \mathbf{f}(\mathbf{x},t), \tag{2}$$

$$0 = \nabla\cdot\mathbf{u}(\mathbf{x},t), \tag{3}$$

where p is the pressure of the flow field, ν is the viscosity of the fluid, Δ is the spatial Laplacian operator, and $\mathbf{f}$ is an external force that effects the fluid. Often vortices are associated to local minima of the pressure field, which are zero points of the pressure gradient. Assuming that the variation of the pressure gradient dominates the changes of the right hand side of the Navier-Stokes equation, it can be expected that also the magnitude of the acceleration has a local minimum in the vicinity of the pressure minimum. Hence, the minima of the acceleration magnitude form a superset of the minima of the pressure. As stated by Kasten et al. [13], the minima of the acceleration magnitude can represent saddles and vortices as features of the velocity field. To exclude saddle like acceleration minima from this set the Jacobian of the velocity field is employed, which can be interpreted as a filtering. For a comparison of the acceleration magnitude to other quantities, we refer to Fuchs et al. [5].

After this general discussion we focus on two illustrative examples: the Oseen and the Lundgren vortex.

The *Oseen vortex model* is a simple textbook model depicting a line vortex that decays due to viscosity and that obeys the incompressible Navier-Stokes equations. In the context of fluid dynamics, it is used as an elementary model in the vortex system of the boundary layer. The velocity V_Θ in the circumferential direction θ is given by

$$V_\Theta(r) = \frac{\Gamma}{2\pi}\,\frac{1-e^{-(\frac{r}{r_c})^2}}{r}, \tag{4}$$

where r is the spatial coordinate with origin in the center of the vortex, r_c is a parameter determining the core radius and the parameter Γ is the circulation contained in the vortex. For further information, we refer to Rom-Kedar et al. [23] or Noack et al. [15]. In a nutshell, the Oseen vortex is formed by a single center point in the spatial domain surrounded by particles that are circling around this point. While this

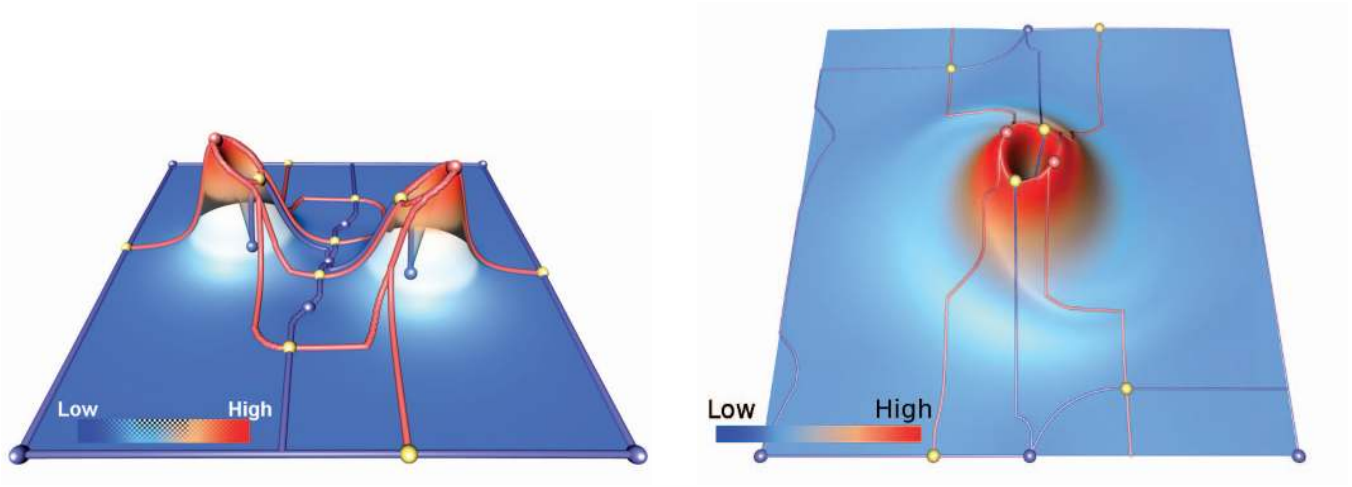

(a) Two co-rotating Oseen vortices.

(b) Lundgren vortex: a non-circular vortex model.

Fig. 2. Acceleration magnitude for two vortex models displayed as colored height field over the flow domain. The topology of the acceleration magnitude is displayed by blue (minima), yellow (saddles), and red (maxima) spheres and the corresponding extremal lines; minima and maxima lines are shown as blue and red lines, respectively. In both cases the minima, representing the vortex core, are surrounded by clearly pronounced ridges.

idea of a vortex is quite simple, it is suitable for several definitions of vortices. Fig. 2(a) shows the acceleration for two co-rotating Oseen vortices using a heightfield superposed by the associated scalar field topology. Thereby, the spheres depict minima (blue), saddles (yellow) and maxima (red). The red and blue lines show the maxima and minima lines respectively.

The *Lundgren vortex model* [14] is an example for a non-circular basic vortex. It also is a solution of the Navier-Stokes equations. Lundgren has shown that solutions of the two-dimensional Navier-Stokes equations can be lifted to three dimensions using the Lundgren transformation. In his paper, he used this vortex as an example. In Fig. 2(b), the acceleration of a discrete Navier-Stokes (DNS) computation [32] of this vortex is depicted.

We observed for the Oseen as well as for the Lundgren vortex that the minima corresponding to vortex cores are enclosed by pronounced ridges in the acceleration magnitude field. This is a typical structure that can also be found in other flows, e.g., in the flow behind a circular cylinder, as shown in Fig. 1. This observation leads to the new definition of a vortex region as the area containing a vortex-like minimum of the acceleration bounded by the corresponding ridge.

In terms of topology, this region is called the *basin of the minimum*. It is bounded by the associated maxima lines, which separate the minimum from other minima in the field. This definition of the vortex region is parameter-free. Due to its topological foundation, the boundary of the regions can be arbitrarily shaped. Note that for each minimum in the topology one such region exists. Thus, it is important to restrict the definition to minima that were extracted using the above mentioned Jacobian filter criterion.

Note that the notion of vortex regions is inherently vague. For arbitrary vortices, the region of rotational flow behavior can be infinite, as in the example of the Oseen vortex. Thus, each definition of vortex regions has to settle on criteria which respect a certain perspective. Our definition of a vortex region is driven by the following conditions:

- being Galilean invariant;
- reflecting Lagrangian particle motion;
- being formulated in consistency with vortex cores;
- being independent from any threshold value;
- allowing vortex regions of arbitrary shape.

4 Algorithm

Algorithmic overview – In this section, we describe how we can robustly extract the vortex regions proposed in Sec. 3. In the following, the algorithmic pipeline as shown in Fig. 3 is briefly summarized. The input of the method is of a two-dimensional, time-dependent vector field. The first step is to compute the magnitude of the acceleration of this field, from which minima are extracted using the robust topological framework provided by Reininghaus et al. [21]. A Jacobian filter classifies the minima into vortex- and saddle-like. The remaining minima are then tracked using combinatorial feature flow fields (CFFF) as presented in [22]. This framework also comprises a spatio-temporal importance measure, which can be used to remove spurious structures. For each time step the vortex regions, the associated basins of the minima, are determined using the same algorithmic framework as for the minima extraction. Finally, a triangulated surface is generated, which connects the individual boundary lines using an advancing front scheme in a postprocessing step.

Minima extraction and tracking – The algorithmic challenge is to robustly extract and track the topological structure of the acceleration field. Acceleration is a derivative of the vector field data. Typically, differentiation of simulated or measured data amplifies noise and therefore usually creates many spurious extremal structures. These structures severely affect both aforementioned steps of the algorithmic pipeline: Vortex core lines are interrupted and vortex regions suffer from topological oversegmentation.

A method dealing well with these challenges is the utilization of combinatorial feature flow fields (CFFF), as proposed in [22]. The basic idea of CFFF is to compute a sequence of combinatorial gradient vector fields to represent the input data using computational discrete Morse theory. This allows for a simplification of the combinatorial gradient vector fields using persistence to remove spurious structures. The minima (critical points of the gradient vector field) are then tracked in this sequence with combinatorial algorithms. Further, this approach provides an importance measure for the tracked minima that can be summarized as integrated persistence. It extends the idea of feature lifetime proposed in [13]. In our setting, this measure allows us to build a hierarchy of vortex core lines of the given time-dependent vector field. Note that the above-mentioned simplification using persistence is essential in our context, since a topological oversegmentation would not result in the correct vortex regions.

Vortex region extraction – The vortex regions are defined as the associated basins to the acceleration minima and as such are also part of the scalar field topology. Thus they can be extracted using the same frame-

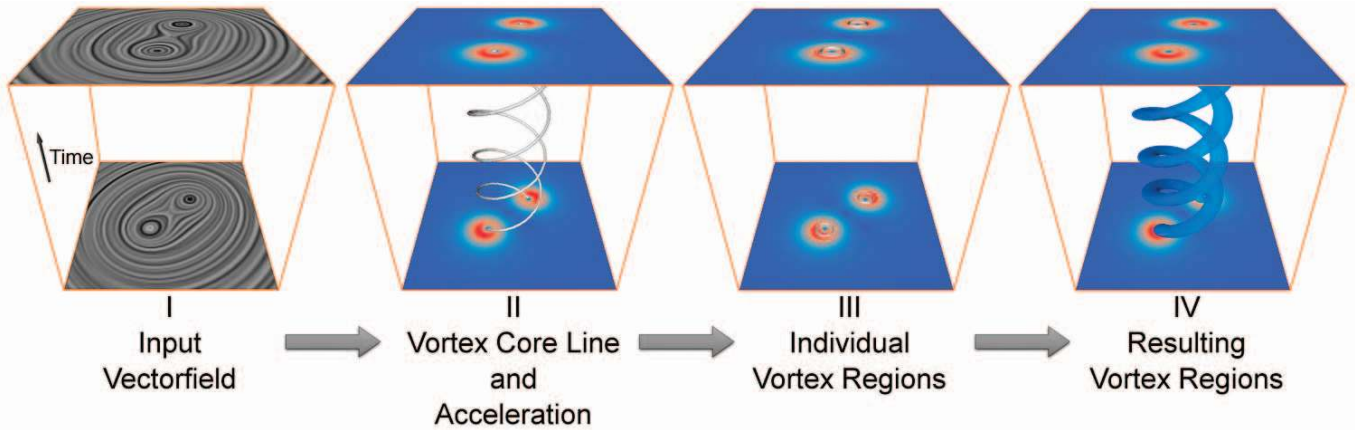

Fig. 3. Overview of the vortex region extraction pipeline. (I) As input, a time-dependent vector field is used. (II) The acceleration magnitude and its topology is computed using robust algorithms. The minima depicting vortex cores are tracked over time. (III) The individual vortex regions for each slice are computed. (IV) The tracking is used to connect the region boundaries.

Algorithm 1 Main vortex region algorithm

Input: Vortex core lines C, Topological skeletons T
Output: VortexRegions R

R = getVortexRegions(C,T)
1: **for all** $L \in C$ **do**
2: **for all** $P \in L$ **do**
3: $S \leftarrow$ getSkeleton(P, T)
4: $B \leftarrow$ getBasinBoundary(P, S)
5: L.append(B)
6: L.VortexRegions $\leftarrow$ TriangulateRegions(L)

Algorithm 2 Find basin boundary for a single minimum

Input: Minimum P, Topological skeleton T
Output: Basin boundary of minimum B

B = getBasinBoundary(P, S)
1: connSaddles $\leftarrow$ getConnectedSaddle(P, T)
2: **for all** saddle $\in$ connSaddles **do**
3: maxLines $\leftarrow$ getMaxLinesOfSaddle(saddle,T)

work as for the minima computation even though this is not an explicit part of [21]. The resulting topological skeleton, critical points and separatrices, contain all necessary information to extract the basins.

Given the vortex cores represented by minima and the topological skeletons in each time step Algorithm 1 illustrates the general approach. For each point of each time-dependent vortex core line (lines 1,2), we fetch the associated topological skeleton (line 3). We then determine the boundary of its associated basin (line 4) and append these lines to the vortex core line (line 5). Finally, we build a surface from the vortex region lines using a simple advancing front approach that is not further described here (line 6).

The main step, the extraction of the boundary of the basin, is given in Alg. 2. The essential parts of the topological skeleton needed are the saddles connected to the current minimum (line 1) and the maximum lines starting in these saddles (line 2,3). This behavior is illustrated in Fig. 1: minima (blue), saddles (yellow), maxima (red), and the maxima lines (black). One basin boundary is highlighted as white line. Note that the minima lines (blue) connecting the minima with the saddles are only displayed for the highlighted region. The minima not depicting vortices are crossed out.

5 Implementational Details

To achieve a good reproducibility of the results shown in this paper, this section presents three implementational aspects.

We employ the combinatorial framework described in Reininghaus et al. [21]. In this framework, the extraction of the saddles connected to the minima is quite simple. The scalar field is represented as a combinatorial gradient field, which is defined as a matching on a cell graph. The basin of a minimum can be extracted by doing a breadth-first search in the graph. Thereby, the search path has to be alternating with respect to the matching. The maxima lines are then extracted by integrating a combinatorial streamline.

Note that the maxima lines in a combinatorial gradient vector field can share edges in the cell graph. To get the boundary without these artifacts, we need to discard these parts of the maxima lines. Therefore, we remove the points of the lines that are present twice in one vortex region.

As the combinatorial streamlines can only follow the edges of the given cell graph, the resulting vortex regions are not smooth enough for an efficient visual perception of the generated surfaces. Therefore, we apply a smoothing step to the resulting boundary lines before we construct the surface. For a depiction of this postprocessing step, we refer to Fig. 4.

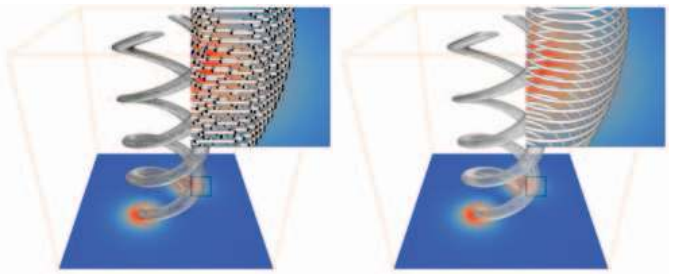

Fig. 4. Individual vortex region boundaries for the dataset of two co-rotating Oseen vortices. Due to the combinatorial approach for the region extraction, a postprocessing of the extracted vortex region boundary is necessary to achieve a good visual quality.

6 Results

We apply our algorithm for extracting vortex regions to three different datasets. Since all flows considered in this paper are planar and non-stationary, we depicted time as third dimension.

Co-rotating Oseen vortices – The first data set is our model example of two co-rotating Oseen vortices, see Fig. 6. At the bottom, the acceleration is encoded in color. Thereby, red indicates high and blue low acceleration. There are two blue pipes emanating from the bottom slice that show the evolution of the circular region. Within the transparent pipes, the tracked vortex core lines can be seen. The regions are

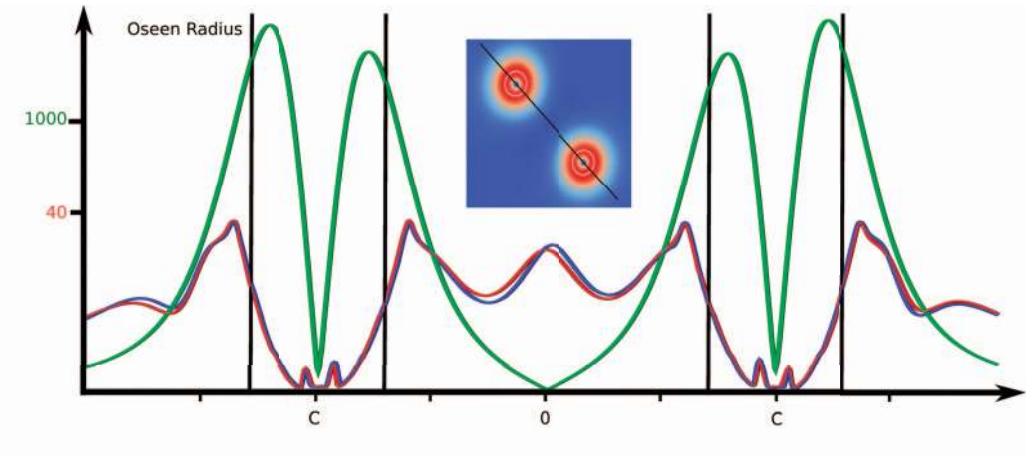

Fig. 5. Plot of the forward (red) and backward (blue) FTLE and the acceleration magnitude (green) for a cut in the domain of the Oseen dataset as shown in the image. The values are sampled on the line shown in the center image. The parameter r_c of the Oseen vortex is also shown (black lines).

correctly tracked over the complete time the core lines exist.

To analyze the relation of the parameter r_c, see Equation 4, in the definition of two co-rotating Oseen vortices with the size of our vortex regions, we plotted the acceleration magnitude (green) along a cut on one slice of the dataset, cf. Fig. 5. Additionally, the forward (red) and backward (blue) FTLE values along this line are shown. FTLE is computed for one sixth of a period of the dataset. While the maxima of the acceleration are closer to the vortex center c than the parameter r_c, the maxima of the FTLE are further away.

Cylinder dataset – The next dataset, referred to as the *cylinder* dataset, resulted from a time-dependent 2D CFD simulation of the von-Kármán vortex street [16, 33], the flow behind a cylinder with $Re = 100$. It consists of 32 time steps. The flow is periodic, allowing a temporal unbounded evaluation of the field. In Fig. 7, the vortex regions are depicted for nine shedding periods. The extracted surfaces are colored by the acceleration magnitude. Time is again chosen as third dimension. Red coloring depicts high values and blue low values of the acceleration magnitude. The vortices detach from the cylinder as weak features. Their spatial importance is growing quickly and attenuates in the flow. As can be seen, the regions do not depict a single value of the acceleration. Thus, iso-surface extraction cannot be used to determine the region boundaries.

In Fig. 8, a comparison of different definitions of vortex regions is shown. The minima of the acceleration (red) and the critical points of vector field topology (green) are depicted in each image. To extract the critical points, an appropriate frame of reference was chosen that reveals the typical pattern of the von-Kármán vortex street. Note that directly behind the cylinder the locations of the critical points and the vortex cores differ very much. The revealing frame of reference is not correctly chosen for these points. It depends on the velocity of the vortices, which are slower directly behind the cylinder. Fig. 8 (a) shows the result of our method. The coloring of the slice is determined by the acceleration. It can be seen that the region boundary cannot be determined by an iso-value. Furthermore, the regions get larger with growing distance to the cylinder. Fig. 8 (b)-(c) show iso-values of different scalar quantities that are used to identify vortices. All these quantities are Galilean invariant. First, vorticity is shown. While the size of the outer regions stays nearly constant, the inner regions shrink with growing distance to the cylinder. Directly behind the cylinder, regions of different vortices merge. The second quantity used to identify vortex-like behavior is λ_2. The third quantity is *vortex strength* as introduced by Bauer et al. [3]. This is magnitude of the imaginary part of the complex eigenvalues of the Jacobian matrix. Both quantities show comparable results in size and shape. The size of the outer regions stays constant when moving down the flow and the inner regions shrink. Thus the impression of the development of the vortices strongly depends on the chosen iso-value.

In contrast to the first four definitions, the regions in Fig. 8 (e+f) depend on the chosen frame of reference as well as on the critical points of the vector field topology. The first method searches for the maximum tangential velocity on a fan of rays send out from a critical point. The resulting regions are therefore restricted to star-shaped geometries. Surprisingly, the regions have nearly the same shape and size as the outer regions in Fig. 8(e) and (d). In Fig. 8 (f), the regions are determined by searching closed streamlines in rotated versions of the vector field. The image shows the largest boundaries that can be found beginning at the critical points. The shape of these regions differs most from the other results. Their size stays constant after some initial growth.

Flow over a cavity – A more complex model is the flow over a cavity. The dataset is the result from a numerical simulation of a weakly compressible 2D flow over a cavity at Ma= 0.38, cf. [4]. In Fig. 10, the flow over the cavity (yellow) moves from left to right and time is represented by the third dimension pointing from back to front. This is again a periodic data set of which one period is shown. The acceleration field is displayed by volume rendering (blue). Pathlines, seeded in the vicinity of the extracted vortex core lines (red), exhibit typical vortex behavior, swirling around the tracked minima of the acceleration. The thickness of the core lines encodes the integrated spatial importance, which is the importance measure proposed in [22]. For a good visual perception, we focused on the three most important vortex core lines. The blue surfaces depict the boundaries of the vortex regions extracted with our method. It can been observed that the region of the central vortex core line is growing as the vortex detaches from the leading edge and moves through the cavity over the trailing edge.

Comparison to FTLE – In Figure 9, the computed finite-time Lyapunov exponent (FTLE) for the different datasets is shown. FTLE measures the separation of infinitesimal close particles over a finite time period, as proposed by Haller [8]. In the image, the blue coloring shows backward FTLE that corresponds to convergence of particles and the red coloring depicts forward FTLE that corresponds to separation. The vortex regions extracted from the acceleration magnitude of this slice are added to the image. In Fig. 9 (a), the ridges of both forward and backward FTLE of the co-rotating Oseen vortices enclose the vortex region. While the shape of the extracted vortex region boundary is similar, the size is smaller. This can also be seen in the plot shown in Fig. 5. The same observation can be made for the cavity in Fig. 9 (b). Here, especially the backward FTLE ridges (blue) correspond to the

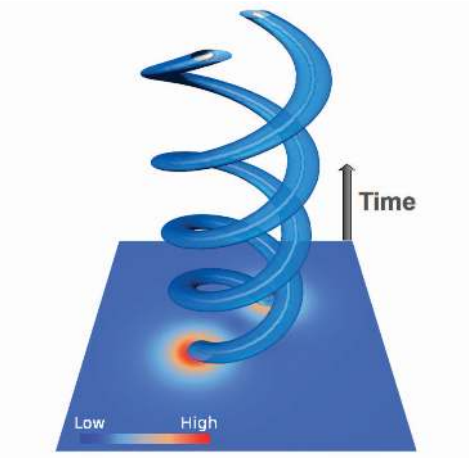

Fig. 6. Tracked vortex regions of the Oseen dataset. At the bottom, the acceleration is shown. The vortices are depicted by their cores (white lines) and the boundary of the regions (blue).

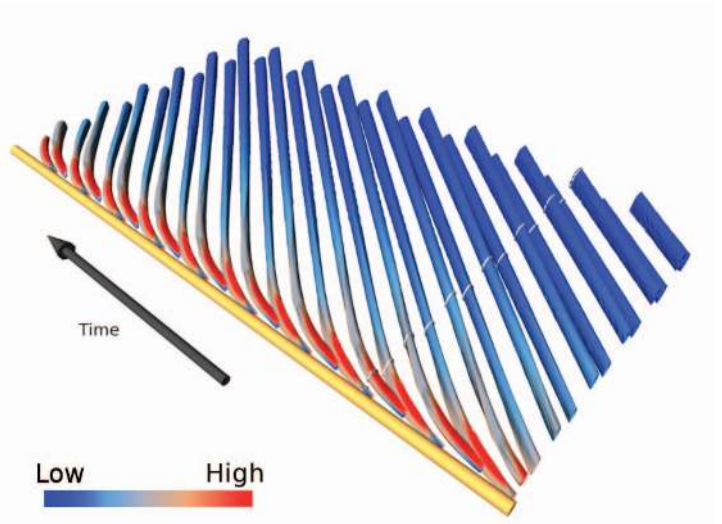

Fig. 7. Tracked vortex regions of the cylinder dataset colored by the acceleration magnitude. Red coloring depicts high values and blue low values. Due to the different scalar values on the surface, these regions cannot be determined by iso-surface extraction. The white rings enclosing the vortex regions refer to the time slice shown in Fig. 8 (a) and Fig. 9 (c).

shape of the extracted vortex regions. In Fig. 9 (c), the ridges of the backward FTLE (blue) are similar to the shape as well as the size of the regions.

Note that, given the vortex core lines and the individual combinatorial gradient vector fields, the running time for the extraction of the vortex regions is insignificant. The time to compute the results shown in this paper is therefore given by the time of the vortex core line extraction. For a detailed running time analysis of the combinatorial feature flow field method, we refer to [22].

7 Conclusions and Future Work

This paper proposed a novel vortex region definition based on the extremal structures of the magnitude of the acceleration.

From a theoretical perspective, this definition has three important properties. First, it is independent from the chosen frame of reference of the underlying vector field, since it is based on the acceleration. Furthermore, the vortex regions are not restricted to star- or convex-shaped geometries. Finally, it does not depend on a user specified parameter such as a threshold or an iso-value.

From a practical perspective, the proposed definition allows for an efficient and robust algorithmic treatment as was demonstrated in Sec. 6. Even when the acceleration contains a lot of spurious structures as in the dataset shown in Fig. 10, we are able to reliably extract the vortex cores and corresponding vortex regions.

The definition of vortex regions based on the topological skeleton of the acceleration magnitude can in principle be transferred to three dimensions. Anyhow, a few things should be analyzed first: Which topological structures of the acceleration magnitude represent vortices in three dimensions? In which way can these structures be tracked over time efficiently? Which topological structures can be used to define the boundary of a vortex based on the acceleration magnitude? The answers to the domain specific questions may be similar. It seems sensible that in three dimensions vortex centerlines are described by the minima lines of the acceleration magnitude and the vortex cores are given by the associated basins of the minima. On the other side, the extension of the used tracking algorithm (CFFF) to three dimensions is much more complicated. The solution of this problem needs much more investigation.

As can be observed in Fig. 9, the ridges of the backward FTLE field correlate with the boundaries of our vortex regions which are based on the acceleration magnitude. As stated by Shadden [26], ridges of the FTLE field depict Lagrangian coherent structures, which are fundamental features of time-dependent flow fields. It will be interesting to further analyze this interrelationship of extremal structures of the acceleration magnitude and the extremal structures of the FTLE.

Acknowledgments

The project is supported by the DFG. The authors wish to thank Bernd Noack for fruitful discussions, Oliver Kamps for providing the Lundgren dataset, Gerd Mutschke for providing the cylinder dataset, and Mo Samimy for providing the cavity dataset. All visualizations have been created using Amira – a system for advanced visual data analysis (`http://amira.zib.de`).

References

[1] D. C. Banks and B. A. Singer. A predictor-corrector technique for visualizing unsteady flow. *IEEE Transactions on Visualization and Computer Graphics*, 1(2):151–163, 1995.

[2] D. Bauer and R. Peikert. Vortex tracking in scale-space. In D. Ebert, P. Brunet, and I. Navazo, editors, *VisSym02 Joint Eurographics - IEEE TCVG Symposium on Visualization*, pages 233–240. Eurographics Association, 2002.

[3] D. Bauer, R. Peikert, M. Sato, and M. Sick. A case study in selective visualization of unsteady 3d flow. In *VIS '02: Proceedings of the Conference on Visualization '02*, pages 525–528, Washington, DC, USA, 2002. IEEE Computer Society.

[4] E. Caraballo, M. Samimy, and J. DeBonis. Low dimensional modeling of flow for closed-loop flow control. In *AIAA Paper*, volume 59, 41st AIAA Aerospace Science Meeting, January 6-9, 2003, Reno, NV, USA.

[5] R. Fuchs, J. Kemmler, B. Schindler, J. Waser, F. Sadlo, H. Hauser, and R. Peikert. Toward a Lagrangian vector field topology. *Computer Graphics Forum*, 29(3):1163–1172, June 2010.

[6] C. Garth, X. Tricoche, T. Salzbrunn, T. Bobach, and G. Scheuermann. Surface Techniques for Vortex Visualization . In O. Deussen, C. Hansen, D. Keim, and D. Saupe, editors, *Symposium on Visualization*, pages 155–164, Konstanz, Germany, 2004. Eurographics Association.

[7] C. Garth, X. Tricoche, and G. Scheuermann. Tracking of vector field singularities in unstructured 3d time-dependent datasets. In *In Proc. IEEE Visualization 2004*, pages 329–336, 2004.

[8] G. Haller. Distinguished material surfaces and coherent structures in three-dimensional fluid flows. *Physica D*, 149(4):248–277, 2001.

[9] G. Haller. An objective definition of a vortex. *Journal of Fluid Mechanics*, 525:1–26, 2005.

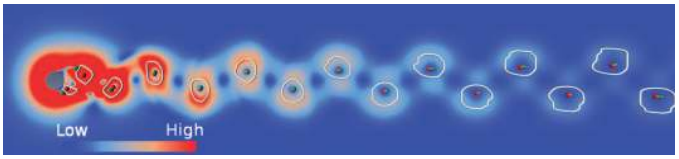

(a) Our Method

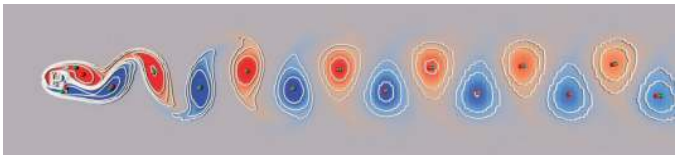

(b) Vorticity Iso-lines

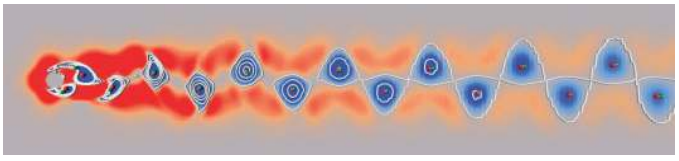

(c) λ_2 Iso-lines [27]

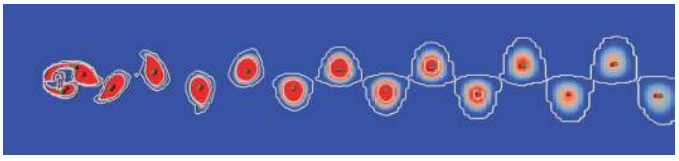

(d) Vortex Strength [3]

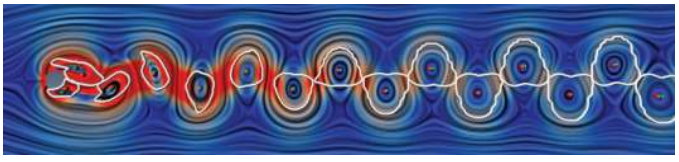

(e) Tangential Velocity Maximum [6]

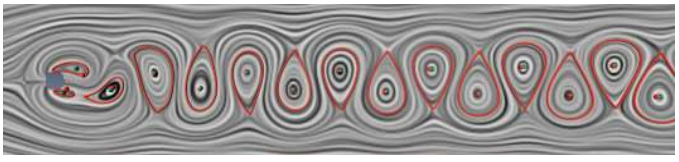

(f) Vortex Regions based on Streamlines [17]

Fig. 8. Comparison of different definitions of vortex regions, computed for the cylinder dataset. The coloring of the slices is determined by the quantity the regions are based on. In all figures, the critical points (green) of vector field topology are depicted. The red points are the minima of the acceleration magnitude depicting vortex cores. Fig. (a) shows the result of our method based on the acceleration. Fig (b)-(d) show iso-lines of vorticity (b), λ_2 (c), and vortex strength (d) as defined by Bauer et al. [3]. In Fig. (e), the regions are determined by searching the maximum tangential velocity sending out a fan of rays from the critical points. The coloring of the LIC is determined the velocity magnitude. Fig. (f) shows the result of the streamline based method.

[10] J. Hunt. Vorticity and vortex dynamics in complex turbulent flows. *Trans. Can. Soc. Mech. Eng.*, 11:21–35, 1987.
[11] M. Jankun-Kelly, M. Jiang, D. Thompson, and R. Machiraju. Vortex visualization for practical engineering applications. *IEEE Transactions on Visualization and Computer Graphics*, 12(5):957–964, 2006.
[12] J. Jeong and F. Hussain. On the identification of a vortex. *Journal of Fluid Mechanics*, 285:69–94, 1995.
[13] J. Kasten, I. Hotz, B. Noack, and H.-C. Hege. On the extraction of long-living features in unsteady fluid flows. In V. P. et al., editor, *Topological Methods in Data Analysis and Visualization. Theory, Algorithms, and Applications.*, Mathematics and Visualization, pages 115–126. Springer, 2011.
[14] T. S. Lundgren. Strained spiral vortex model for turbulent fine structure. *Physics of Fluids*, 25(12):2193–2203, 1982.
[15] B. Noack, I. Mezić, G. Tadmor, and A. Banaszuk. Optimal mixing in recirculation zones. *Physics of Fluids*, 16(4):867–888, 2004.
[16] B. R. Noack, M. Schlegel, B. Ahlborn, G. Mutschke, M. Morzyński, P. Comte, and G. Tadmor. A finite-time thermodynamics of unsteady fluid flows. *Journal Non-Equilibrium Thermodynamics*, 33(2):103–148, 2008.
[17] C. Petz, J. Kasten, S. Prohaska, and H.-C. Hege. Hierarchical vortex regions in swirling flow. *Computer Graphics Forum*, 28(3):863 – 870, 2009.
[18] A. Pobitzer, R. Peikert, R. Fuchs, B. Schindler, A. Kuhn, H. Theisel, K. Matkovic, and H. Hauser. On the way towards topology-based visualization of unsteady flow - the state of the art. In *EuroGraphics 2010 State of the Art Reports (STARs)*, pages 137–154, 2010.
[19] F. H. Post, B. Vrolijk, H. Hauser, R. S. Laramee, and H. Doleisch. The state of the art in flow visualisation: Feature extraction and tracking. *Computer Graphics Forum*, 22(4):775–792, 2003.
[20] F. Reinders, I. Sadarjoen, B. Vrolijk, and F. Post. Vortex tracking and visualisation in a flow past a tapered cylinder. *Computer Graphics Forum*, 21(4):675–682, 11 2002.
[21] J. Reininghaus, D. Günther, I. Hotz, S. Prohaska, and H.-C. Hege. TADD: A computational framework for data analysis using discrete Morse theory. In *Mathematical Software – ICMS 2010, volume 6327 of Lecture Notes in Computer Science*, pages 198–208. Springer, 2010.
[22] J. Reininghaus, J. Kasten, T. Weinkauf, and I. Hotz. Efficient computation of combinatorial feature flow fields. *IEEE Transactions on Visualization and Computer Graphics*, 2011 (to appear).
[23] V. Rom-Kedar, A. Leonard, and S. Wiggins. An analytical study of transport, mixing and chaos in an unsteady vortical flow. *Journal of Fluid Mechanics*, 214:347–394, 1990.
[24] I. A. Sadarjoen and F. H. Post. Geometric methods for vortex extraction. In *Joint Eurographics-IEEE TVCG Symposium on Visualization*, pages 53–62, 1999.
[25] D. Schneider, A. Wiebel, H. Carr, M. Hlawitschka, and G. Scheuermann. Interactive comparison of scalar fields based on largest contours with applications to flow visualization. *IEEE Trans Vis Comput Graph*, 14(6):1475–1482, 2008.
[26] S. C. Shadden. *A Dynamical Systems Approach to Unsteady Systems*. PhD thesis, California Institute of Technology, Pasadena CA, 2006.
[27] S. Stegmaier, U. Rist, and T. Ertl. Opening the Can of Worms: An Exploration Tool for Vortical Flows. In C. Silva and E. Gröller and H. Rushmeier, editor, *Proceedings of IEEE Visualization '05*, pages 463–470. IEEE, 2005.
[28] P. Tabeling. Two-dimensional turbulence: a physicist approach. *Physics Reports*, 362(1):1 – 62, 2002.
[29] H. Theisel and H.-P. Seidel. Feature flow fields. In *VisSym '03: Proceedings of the Symposium on Data Visualization 2003*, pages 141–148, Aire-la-Ville, Switzerland, 2003. Eurographics Association.
[30] A. Tikhonova, C. D. Correa, and K.-L. Ma. An exploratory technique for coherent visualization of time-varying volume data. *Computer Graphics Forum*, 29(3):783–792, 2010.
[31] X. Tricoche, T. Wischgoll, G. Scheuermann, and H. Hagen. Topology tracking for the visualization of time-dependent two-dimensional flows. *Computer & Graphics*, 26:249–257, 2002.
[32] M. Wilczek, O. Kamps, and R. Friedrich. Lagrangian investigation of two-dimensional decaying turbulence. *Physica D: Nonlinear Phenomena*, 237(14-17):2090 – 2094, 2008.
[33] C. H. K. Williamson. Vortex dynamics in the cylinder wake. *Annual Review of Fluid Mechanics*, 28:477–539, 1996.

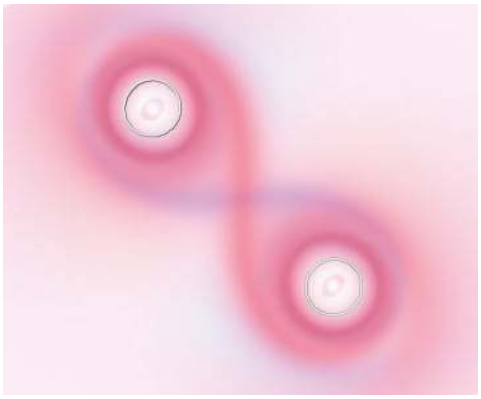

(a) Oseen

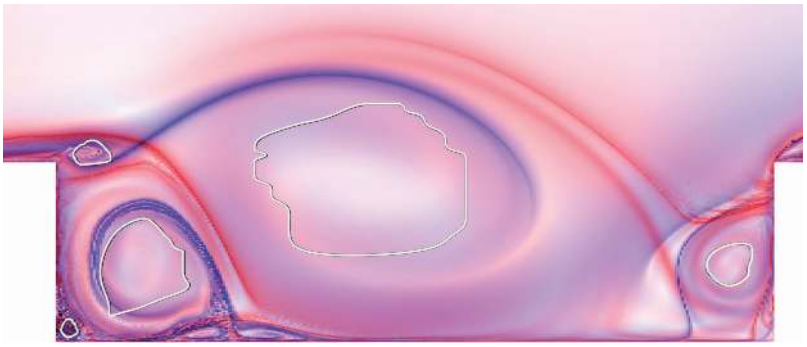

(b) Cavity

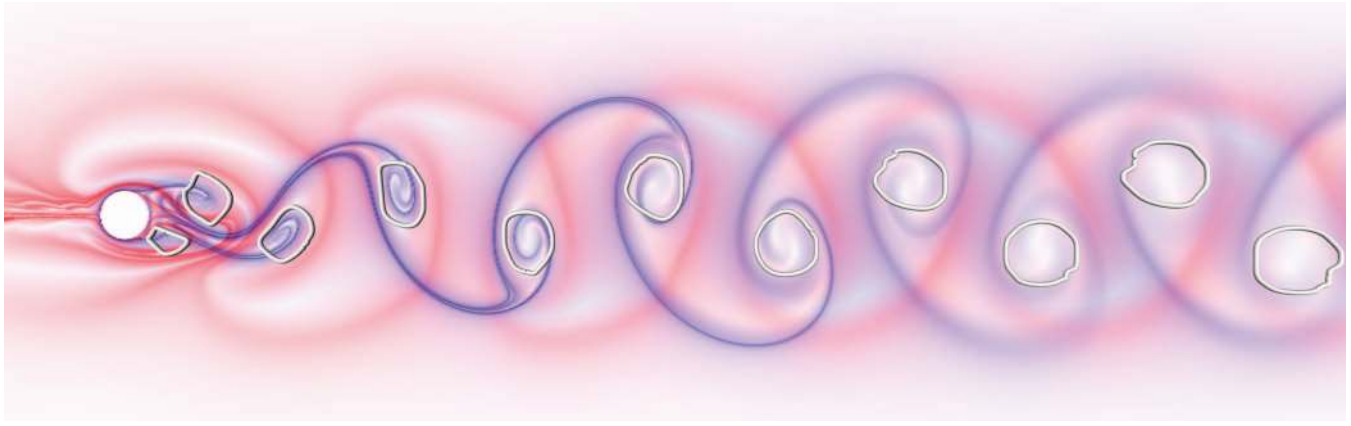

(c) Cylinder

Fig. 9. Forward (red) and backward (blue) FTLE for the Oseen (a), Cavity (b), and Cylinder (c) datasets. For the Oseen vortex pair, the FTLE was computed for the sixth part of a period; the FTLE was calculated for the fifth part of a period for the cavity; and for the cylinder the FTLE was computed for two shedding periods. The vortex regions for these datasets are depicted additionally. A correlation especially between the ridges of the backward FTLE and the vortex regions can be seen.

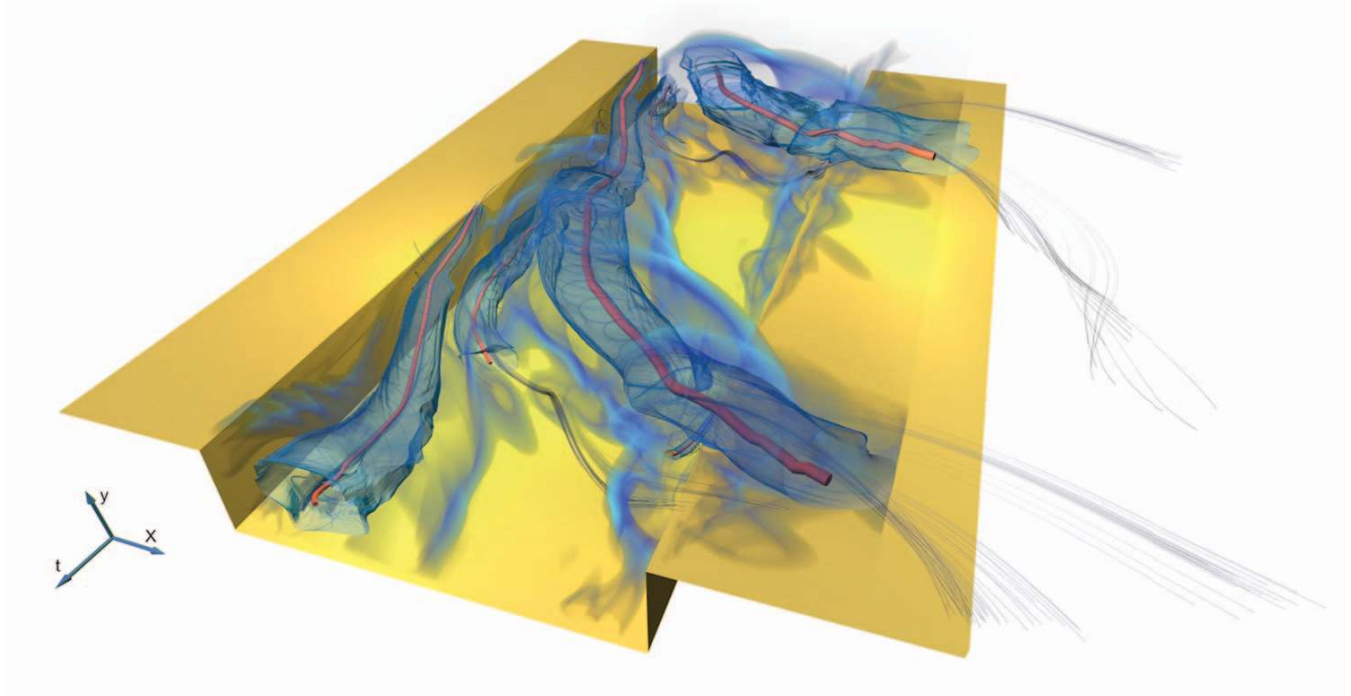

Fig. 10. Time-dependent vortex core lines (red) and their associated vortex regions (blue) extracted for the dataset of a cavity. The acceleration is depicted as volume rendering. Additionally, two kinds of path lines are depicted: the first ones are seeded directly at the extracted vortex core lines and the other are seeded in the vicinity.